

**Final results from the EU project AVATAR**  
**Aerodynamic modelling of 10 MW wind turbines**

Schepers, J. G.; Boorsma, K.; Sorensen, N.; Voutsinas, V.; Sieros, G.; Rahimi, H.; Heisselmann, H.; Jost, E.; Lutz, T.; Maeder, T.

**DOI**

[10.1088/1742-6596/1037/2/022013](https://doi.org/10.1088/1742-6596/1037/2/022013)

**Publication date**

2018

**Document Version**

Final published version

**Published in**

Journal of Physics: Conference Series

**Citation (APA)**

Schepers, J. G., Boorsma, K., Sorensen, N., Voutsinas, V., Sieros, G., Rahimi, H., Heisselmann, H., Jost, E., Lutz, T., Maeder, T., Gonzalez, A., Ferreira, C., Stoevesandt, B., Barakos, G., Lampropoulos, N., Croce, A., & Madsen, J. (2018). Final results from the EU project AVATAR: Aerodynamic modelling of 10 MW wind turbines. *Journal of Physics: Conference Series*, 1037(2), Article 022013. <https://doi.org/10.1088/1742-6596/1037/2/022013>

**Important note**

To cite this publication, please use the final published version (if applicable).  
Please check the document version above.

**Copyright**

Other than for strictly personal use, it is not permitted to download, forward or distribute the text or part of it, without the consent of the author(s) and/or copyright holder(s), unless the work is under an open content license such as Creative Commons.

**Takedown policy**

Please contact us and provide details if you believe this document breaches copyrights.  
We will remove access to the work immediately and investigate your claim.

PAPER • OPEN ACCESS

## Final results from the EU project AVATAR: Aerodynamic modelling of 10 MW wind turbines

To cite this article: J.G. Schepers *et al* 2018 *J. Phys.: Conf. Ser.* **1037** 022013

View the [article online](#) for updates and enhancements.

### Related content

- [Latest results from the EU project AVATAR: Aerodynamic modelling of 10 MW wind turbines](#)  
J.G. Schepers O. Ceyhan, K. Boorsma, A. Gonzalez et al.
- [Numerical analysis of unsteady aerodynamics of floating offshore wind turbines](#)  
M. Cormier, M. Caboni, T. Lutz et al.
- [Development and application of a dynamic stall model for rotating wind turbine blades](#)  
B F Xu, Y Yuan and T G Wang



**IOP | ebooks™**

Bringing you innovative digital publishing with leading voices  
to create your essential collection of books in STEM research.

Start exploring the collection - download the first chapter of  
every title for free.

## Final results from the EU project AVATAR: Aerodynamic modelling of 10 MW wind turbines

J.G. Schepers<sup>1</sup>, K. Boorsma<sup>1</sup>, N. Sørensen<sup>2</sup>, Voutsinas<sup>3</sup> and G Sieros<sup>3</sup>, H. Rahimi<sup>4,9</sup>, H. Heisselmann<sup>4</sup>, E. Jost and T. Lutz<sup>5</sup>, T. Maeder<sup>6</sup>, A. Gonzalez<sup>7</sup>, C. Ferreira<sup>8</sup>, B. Stoevesandt<sup>9</sup>, G. Barakos<sup>10</sup>, N. Lampropoulos<sup>11</sup>, A. Croce<sup>12</sup>, J. Madsen<sup>13</sup>

<sup>1</sup>ECN, Westerduinweg 3, 1755 LE Petten, The Netherlands

<sup>2</sup>DTU, Frederiksborgvej 399, 4000, Roskilde, Denmark

<sup>3</sup>NTUA, P.O. Box 64070, 15710 Zografou, Athens, Greece

<sup>4</sup>ForWind, Kuepkersweg 70, 26129 Oldenburg, Germany

<sup>5</sup>University Stuttgart, Pfaffenwaldring 21, 70569 Stuttgart, Germany

<sup>6</sup>GE, FreisingerLandstrasse 50, 85748, Garching bei Muenchen, Germany

<sup>7</sup>CENER, C/ Ciudad de la Innovación 7, 31621 Sarriguren, España

<sup>8</sup>TU Delft, Kluyerweg 1, 2629 HS Delft, The Netherlands

<sup>9</sup>Fraunhofer IWES, Am Seedeich 45, 27572, Bremerhaven, Germany

<sup>10</sup>University of Glasgow, Scotland

<sup>11</sup>CRES, 19<sup>th</sup> km Marathonos Ave., 19009 Pikermi Attiki, Greece

<sup>12</sup>Polimi, Via La Masa 34, 20156 Milano, Italy

<sup>13</sup>LM Wind Power, AageSkouboesvej, 6640, Lunderskov, Denmark

E-mail: schepers@ecn.nl

**Abstract.** This paper presents final results from the EU project AVATAR in which aerodynamic models are improved and validated for wind turbines on a scale of 10 MW and more. Special attention is paid to the improvement of low fidelity engineering (BEM based) models with higher fidelity (CFD) models but also with intermediate fidelity free vortex wake (FVW) models. The latter methods were found to be a good basis for improvement of induction modelling in engineering methods amongst others for the prediction of yawed cases, which in AVATAR was found to be one of the most challenging subjects to model. FVW methods also helped to improve the prediction of tip losses. Aero-elastic calculations with BEM based and FVW based models showed that fatigue loads for normal production cases were over predicted with approximately 15% or even more. It should then be realised that the outcome of BEM based models does not only depend on the choice of engineering add-ons (as is often assumed) but it is also heavily dependent on the way the induced velocities are solved. To this end an annulus and element approach are discussed which are assessed with the aid of FVW methods. For the prediction of fatigue loads the so-called element approach is recommended but the derived yaw models rely on an annulus approach which pleads for a generalised solution method for the induced velocities.



The paper also discusses uncertainties in the prediction of aero-elastic stability at standstill storm conditions where dependant on the deep stall airfoil data and the dynamic stall model, a stable or instable situation is predicted. For the prediction of deep stall airfoil data DES models were shown to give promising results.

Finally it is concluded that, although AVATAR's strategy to improve lower fidelity models with higher fidelity models was very successful, the experimental validation basis was far too limited. High quality measurements are urgently needed from both field and wind tunnel tests.

## 1. Introduction, objective and approach

This paper presents final recent results from the EU FP7 project AVATAR (AdVanced Aerodynamic Tools of lARge Rotors). AVATAR was initiated by EERA (European Energy Research Alliance) and started in November 2013 and ended in December 2017. The project was carried out in a consortium with 11 research institutes and two industry partners.

- Energy Research Centre of the Netherlands, ECN (Netherlands, coordinator)
- Delft University of Technology, TU Delft (Netherlands)
- Technical University of Denmark, DTU (Denmark)
- Fraunhofer IWES (Germany)
- ForWind - Institute of Physics, University of Oldenburg (Germany)
- University of Stuttgart (Germany)
- National Renewable Energy Centre, CENER (Spain)
- University of Glasgow (UK)
- Centre for Renewable Energy Sources and Saving, CRES (Greece)
- National Technical University of Athens, NTUA (Greece)
- Politecnico di Milano, Polimi (Italy)
- General Electric, GE (Germany)
- LM Wind Power (Denmark)

The focus of the AVATAR project was the aerodynamic modelling of large wind turbines with a rated power of 10 MW or more (denoted as 10MW+ turbines). The rotor designs of such large scale fell outside the validated range of current state-of-the-art aerodynamic and aero-elastic tools in various aspects (e.g. in terms of Reynolds numbers, airfoil thickness, aero-elastic deflections, flow devices etc). Therefore the aim of AVATAR was to improve and validate aerodynamic models, and to ensure their applicability for 10MW+ turbines with and without flow devices, and with and without aero-elastic implications.

To this end, a wide variety of aerodynamic models is considered, ranging from low complexity/computational efficient models (i.e. Blade Element Momentum - BEM) to high fidelity computationally demanding models (e.g. Computational Fluid Dynamics - CFD), with intermediate models (e.g. free vortex wake models FVW) also included. This enables an improvement of the low complexity, fast tools via calibration of their results using high fidelity models. The model assessment is carried out on two 10 MW reference wind turbines (RWT's), one originating from the INNWIND.EU project, and another one designed in AVATAR.

The latter is based on the INNWIND.EU reference turbine [1] but is more challenging in terms of aerodynamic modelling. Aspects like airfoil thicknesses, Reynolds and Mach numbers etc. are pushed towards the limit, i.e. towards more extreme values though still realistic to expect for future commercial applications, see [2].

Furthermore, the improvement and validation of models is based on suitable experimental data, mainly taken in the wind tunnel at e.g. at high Reynolds numbers [3], at turbulent conditions [4], at 360 degrees angle of attack range and on airfoils with flow devices [5] and [6]. A limited number of field measurements on a 2MW turbine were made available from the Danaero experiment [7].

The project finished in December 2017 with a huge number of results which are described in many publications and technical deliverables. These are all publicly available and stored on <http://www.eera-avtar.eu/publications-results-and-links/>.

The number of results is too large to be presented in a single paper. This paper limits itself to a selected number of major findings which are related to model deficiencies and improvements to engineering methods as implemented in design codes. Moreover the paper limits itself to clean blades where clean stands for blades without flow devices even though AVATAR spent a large effort on the modelling of such devices see e.g. [8]. For a more complete overview of the AVATAR results reference is made to the final report [35].

The assessment of engineering methods partly took place by simulating so-called canonical cases with codes of different fidelity, see section 2. These canonical cases are simplified cases, calculated without controller at deterministic yaw, half wake, and shear. In this way insights are obtained in the deficiencies of engineering methods and several of these deficiencies could (partly) be repaired or suggestions for improvements could be given. Section 2 also includes results from full aero-elastic simulations at turbulent inflow. Then section 3 describes model improvements which largely rely on results obtained with ECN's Aero-module. AeroModule is a code which has an easy switch between a BEM based and FVW based model allowing a straightforward comparison of different models using precisely the same input. The section focusses on model improvements for yawed flow and for tip losses. Also the sensitivity of results to the precise implementation of induction modelling is discussed. Finally Section 4 presents results for aero-elastic cases at standstill with emphasis on the sensitivity of results to dynamic stall models and the underlying post stall airfoil data.

## 2. Canonical cases and turbulent inflow cases

The strategy of AVATAR largely relies on using results from high fidelity calculations for the calibration of lower fidelity model. Initially this approach turned out to be problematic because the results from the high fidelity codes suffered from a large spread [10]. Eventually convergent results were obtained from the high fidelity tools by which they were used to calculate a set of (simplified) canonical cases on the AVATAR turbine, the results of which can be found in [10]. The aim of these cases was to condense differences to 'pure' aero modelling effects and to assess the weaknesses and the potential for modelling improvements. The cases had fixed control parameters (fixed pitch and rpm) and they did not include the effect of tower shadowing. The first cases concerned very basic steady axis-symmetric cases after which complexity was added in a systematic way in order to distinguish the modelling effect from separate parameters. The complexity which was added were a yaw angle of 30 degrees, a shear with exponent 0.2 and a half wake based on a cylindrical wake with maximum velocity deficit of 0.35 of the free stream velocity as assumed to be representative for a 5D wake situation. Both a below rated wind speed of 10.5 m/s as well as an above rated wind speed of 14 m/s were considered.

The canonical cases were also calculated in an aero-elastic sense with BEM based models and free vortex wake methods (FVW) with and without flexibility. Apart from canonical cases also full aero-elastic load cases with turbulent input were simulated with both BEM and FVW. The reason why results from FVW instead of CFD codes were used as comparison material for BEM models in an aero-elastic sense lies in the shorter calculational time from FVW methods (an essential argument for long aero-elastic load cases) where FVW models still model induction driven phenomena like yaw,

tip effects and dynamic inflow in a more physical way than BEM based models. Also important to note is that FVW models provide direct information on lifting line variables like the angle of attack and induced velocities. This is not the case for fully resolved CFD which requires specific methods to extract lifting line variables from their output. Several studies on the extraction of lifting line variables were carried out in AVATAR see e.g. [11] and [36] but still some uncertainty remained in all methods which make vortex wake methods a more suitable alternative in case direct information on lifting line variables is needed.

Figures 1 and 2 show a few representative examples for the low wind speed canonical case at half wake conditions and at yawed conditions from these aero-elastic simulations with (anonymous) BEM and Vortex wake methods. Generally speaking it is found (not only for the aero-elastic simulations but also for the CFD simulations of the canonical cases [10]) that the lowest spread is found when the loads are mainly driven by the inflow variation, i.e. the sheared and the half wake case. For the yawed case, the loads are heavily influenced by the induction which leads to a much larger spread. The yaw error in the studied case is 30 degrees, which is large compared to a typical real life situations where the yaw error typically would be less than 10 degrees. The fact that the yaw case is quite extreme, while the shear and half wake situations might be more representative of real life situations, might tend to over emphasize the deviations in this case.

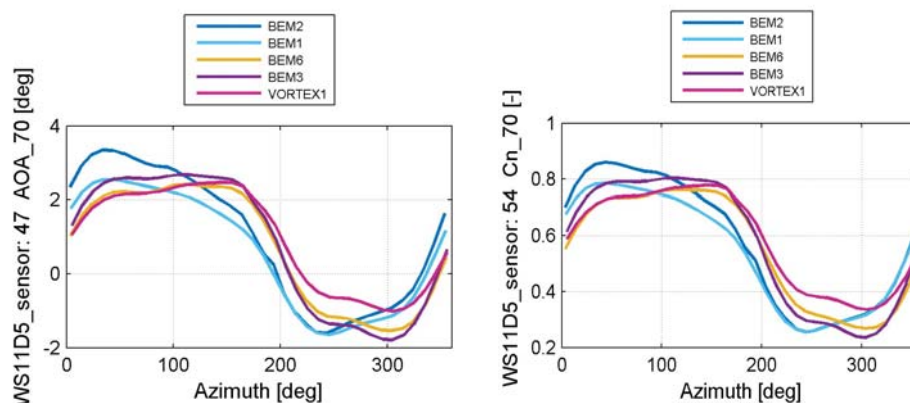


**Figure 1.** Canonical cases: aero-elastic simulation of operation in half wake for the AVATAR RWT. Comparison of the azimuth variation of the angle of attack (left) and the normal to the chord aerodynamic load (right) at the 70% radial station.

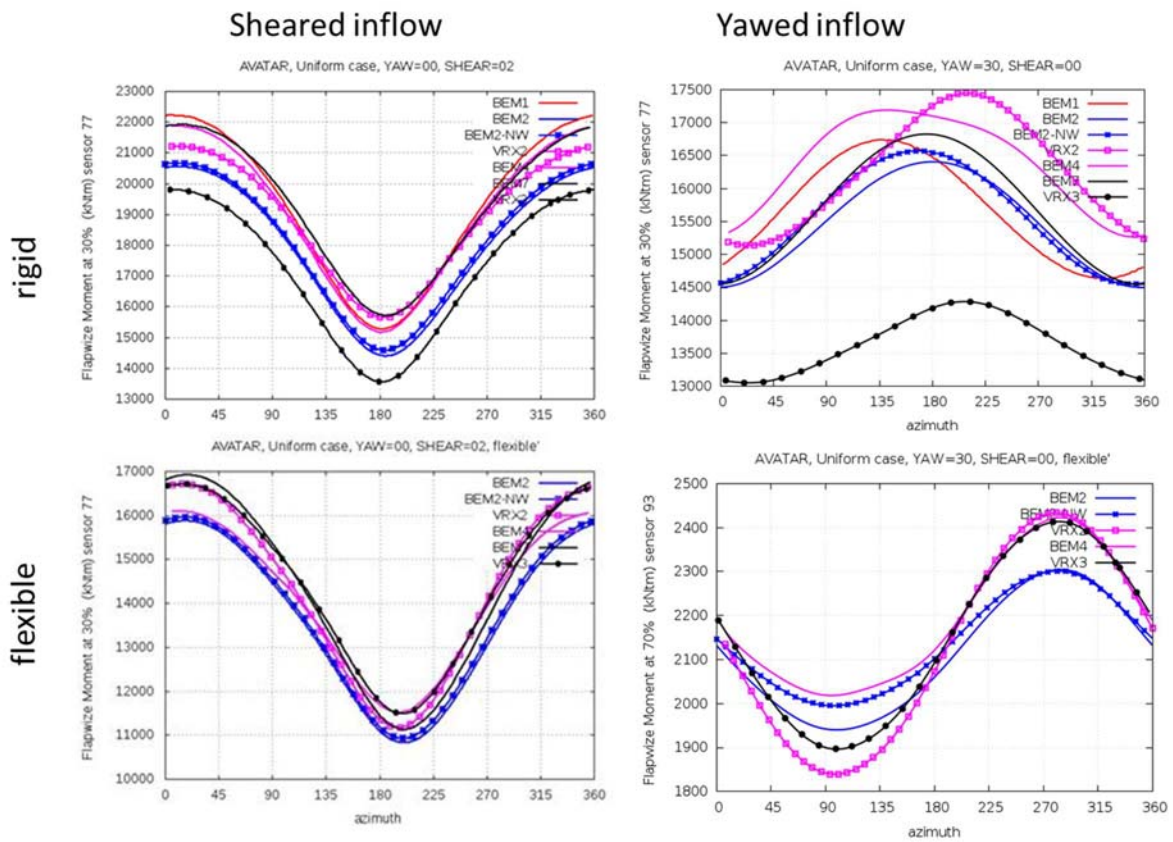


**Figure 2.** Canonical Cases: Operation in sheared (left) and yawed (right) conditions. Comparison of rigid (upper) and flexible (lower) simulations.

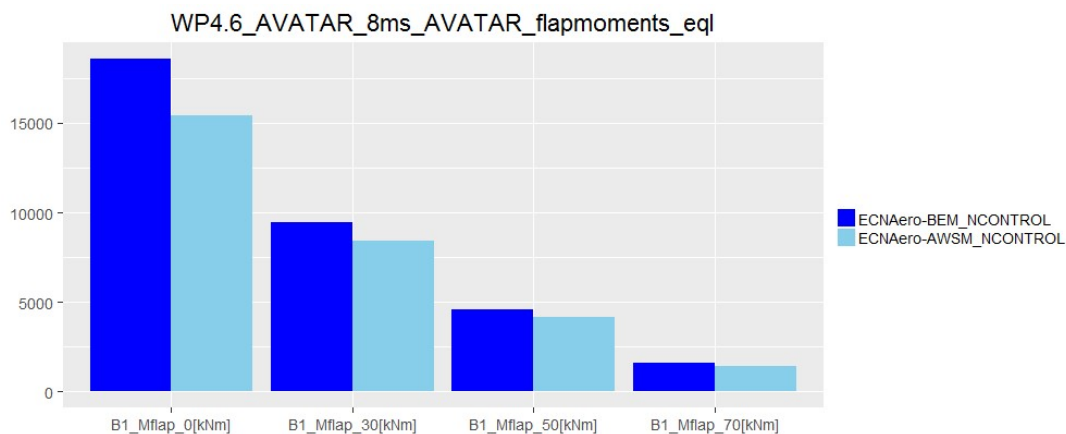


**Figure 3:** Fatigue loads calculated along the blade of the AVATAR RWT at 8 m/s with a BEM code (indicated by ECNAero-BEM-NControl) and a free vortex wake method(indicated by ECNAero-AWSM\_NControl)

Figure 3 shows the equivalent fatigue loads (flap moment) from a full aero-elastic load case with turbulent input largely in agreement with IEC 61400-3. Calculations are performed on the AVATAR RWT at 8 m/s with a BEM and a FVW method as implemented in ECN’s AeroModule (see section 3). The effect of the controller is switched off for better comparison purposes. It can be seen that BEM

overpredicts these loads with 10-20% compared to the FVW method. It is noted that comparisons from [31] with different BEM and vortex methods show similar over predictions from BEM.

This is explained by a more local tracking of the induced velocity variations in FVW models, by which they vary synchronously with the variation in inflow. This synchronization then damps out the variations in angle of attack. Moreover, FVW models allow for a more intrinsic and realistic modelling of shed vorticity variations in time.

### 3. Engineering models: Recommendations and improvements

As explained in section 2, vortex based methods offer a relatively efficient way for a physically accurate modelling of induction effects and so they can be used to improve BEM based codes in that aspect. This will be illustrated with examples which often rely on the ECN AeroModule [16]. AeroModule is a code with an easy switch between the ECN-BEM model and the ECN-AWSM free vortex wake method. Moreover a modified AWSM model is included which prescribes the wake and vortex convection velocities after a certain distance behind the rotor. The AeroModule is coupled to the PHATAS structural solver [17]. In this way the aero-elastic response is calculated with the same input data but with different aero-models in line with the AVATAR philosophy that engineering models are improved using results from more advanced methods. It is emphasized that the main difference between the ECN-BEM and ECN-AWSM model lies in the calculation of induction which is carried out in a more physical way with the vortex approach from AWSM. The effects of airfoil aerodynamics are included in a similar way through airfoil coefficients as function of angle of attack (corrected for three dimensional effects in a similar way). A more physical modelling of airfoil aerodynamics requires more advanced methods like CFD.

#### 3.1. Yawed conditions

As mentioned in section 2 yawed conditions turned out to be one of the most difficult phenomena to predict by engineering methods. Some improvements to the engineering yaw modelling have been made in AVATAR. The starting point for these improvements lied in the observations given in [18] and [19] on the azimuthal variation of induced velocities at yawed conditions which are caused by the skewed wake effect and which were first modelled in the EU projects Dynamic Inflow, see [20]. The models all assumed a sinusoidal variation as induced by a tip vortex wake in line with the model from Glauert leading to stabilizing yawing moments all over the blade.

Later in 1999 Schepers [21] used inflow measurements on a model turbine placed in the TUDelft wind tunnel to develop a new model for the prediction of induction variation with azimuth position. In this work, the measurements of the axial velocity at several radial positions and yaw angles have been expanded in a second-order Fourier series as function of azimuth angle, see equation [1]

$$u_i = u_i(\phi_r) \approx u_{i0} \cdot [ 1 - A_1 \cdot \cos(\phi_r - \psi_1) - A_2 \cdot \cos(2\phi_r - \psi_2) ] [1]$$

The amplitudes  $A_1$  and  $A_2$  and phases  $\psi_1$  and  $\psi_2$  have been tuned as a function of the radial position and yaw angle. In 1999 it was not allowed to publish the precise values of the model parameters but they were in 2012, see [22]. The main difference to the models derived in [20] lies in the inclusion of root vortex effects which were clearly observed in the measurements of velocities in the inner part of the blade. This led to a deviation from the pure sinusoidal behaviour and destabilizing yawing moments at the inner part of the blade. It was interesting to note that in retrospective, the root vortex effects were observed in precisely the same qualitative way in FVW calculations from the National



Technical University of Athens as carried out earlier in the above mentioned Joule projects on Dynamic Inflow.

The 2nd order model with root vortex effects was often found to give significantly better prediction of the loads at yawed conditions than a conventional Glauert based model. This is illustrated in Figure 4 which compares the axial induced velocities at 30 degrees yaw for the INNWIND.EU turbine at 30% and 95% span. Zero azimuth is defined at the 12 o' clock position and yaw is defined such that the so called downwind side of the rotor is between 0 and 180 degrees azimuth.

It can be noted that two BEM models are included: A BEM-Glauert model based on a sinusoidal azimuthal variation of induced velocities all along the blade such that the maximum induced velocity appears at the downwind side of the rotor plane. Moreover results are included from the modified model developed by Schepers indicated with BEM-rv (root vortex). The results are compared with the more physical AWSM free vortex wake and prescribed vortex wake option

Although figure 4 shows that at 30% span both BEM models differ from the AWSM models the qualitative agreement between the BEM-rv model and vortex wake models is good, i.e. the maximum velocity is induced at the upwind side and the minimum velocity is induced at the downwind side. The Glauert model fails to predict this trend, i.e. the maximum induced velocity is reached at the downwind side of the rotor plane as induced by a tip vortex wake only.

On the other hand it can be observed that the qualitative behaviour of the induced velocity at 95% span from the BEM-rv model compares slightly poorer in particular because the dip in induced velocity at an azimuth angle of 90 degrees as a result of the root vortex is still present.

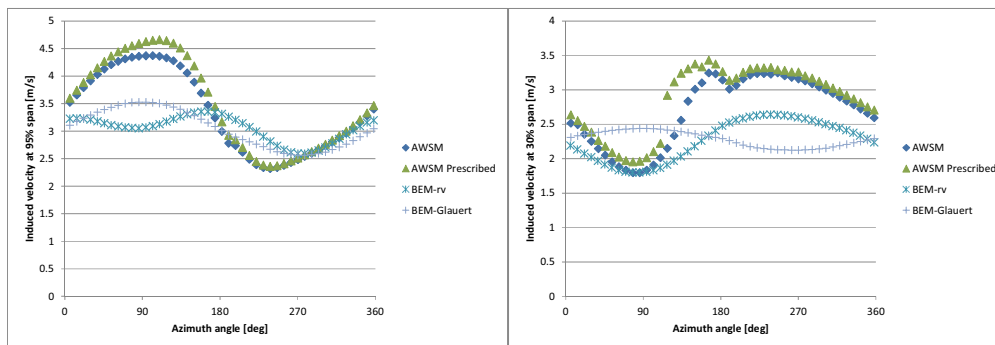
This was explained by the fact that the model from Schepers was tuned on experimental data from a small sized turbine (2 bladed with the rotor diameter of 1.2m) with a strong root vortex. The current wind turbine blades are far bigger and have a smoother transition at the root.

Therefore, in [18] it was suggested to improve Schepers' yaw model by altering the radial dependency of the parameters such that the effect of the root vortex is 'damped out' at 95% span. This was established in a cooperation between ForWind and ECN. The new yaw model was not only based on AWSM results but also on results from an Actuator Line CFD model developed by NREL and used by ForWind [23]. It is noted that the AL-CFD code is not a free vortex wake method but a CFD method but the rotor is modelled as Actuator line approach. The induced velocities from both the AL-CFD and the AL-FVW approach were found to agree extremely well [24])

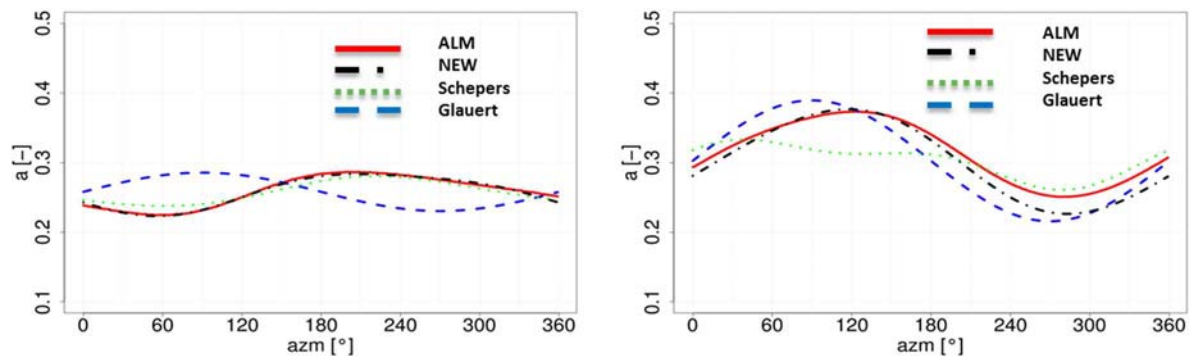
Based on this study a new model was tuned. It is still based on a second order Fourier model but the coefficients have been tuned on the AL-CFD and AL-FVW results for both the AVATAR and INNWIND.EU turbine and also the NREL 5MW Reference Wind turbine.

Figure 5 then shows the results for the induced velocity as function of azimuth angle for the INNWIND.EU turbine. It can be seen that the new model agrees very well with the physical ALM.

It is important to note however that the model from [24] is based on a so-called 'annulus approach' for the induced velocity as represented through the  $u_{i0}$  in equation [1]. In section 3.3 it will be shown that for calculations of turbulent and sheared conditions another approach, a so-called element approach, is preferred.



**Figure 4: Induced velocity as function of azimuth angle at 95% span (left) and 30% span (right) for INNWIND.EU rotor, 6 m/s and 30 degrees yaw**



**Figure 5: INNWIND.EU turbine at 6 m/s and 20 degrees yaw: Induced velocity as function of azimuth angle at 30% span (left) and 80% span (right)**

### 3.2. Tip loss factor

An important simplification in the momentum theory is the representation of the rotor by an actuator disc. Such actuator disc is a hypothetical concept which to some extent can be seen as a rotor with an infinite number of blades since the flow in the rotor plane is assumed to be uniform.

However, the fact that a real rotor has a finite number of blades makes the actual flow in the rotor plane non-uniform.

This non-uniformity is generally covered with the Prandtl tip loss correction  $F$ , (or modifications to it, see [25]). In its basis the Prandtl tip loss factor gives the ratio between the annulus averaged induction in momentum theory and the local axial induction factor at the blade (as applied in the blade element theory) Prandtl derived the factor in the pre-computer era (1919). This necessitated the use of a very simplified vortex wake concept by which it was possible to derive the factor analytically

The simplified model from Prandtl consisted of vortex planes, as given in figure 6 representing the helical vortex sheets behind a finite blade rotor which move with a constant transport velocity  $V_w(1-a)$  without wake expansion and with a mutual distance  $d$ . Flow wipes in and out from the free stream into the stream tube which brings the actual wake velocity near the outer part of the blade between the outer free stream velocity  $V_w$  and the inner wake velocity  $V_w(1-a)$

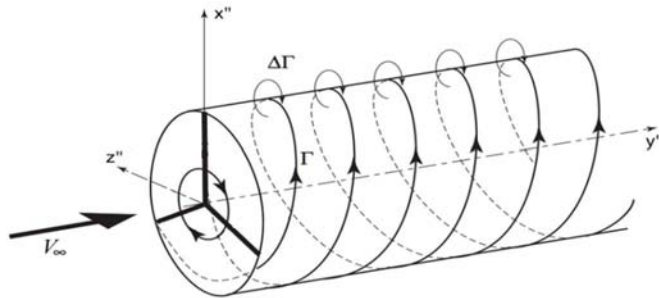


Figure 6: Helical vortex sheet behind a finite bladed rotor (From [26])

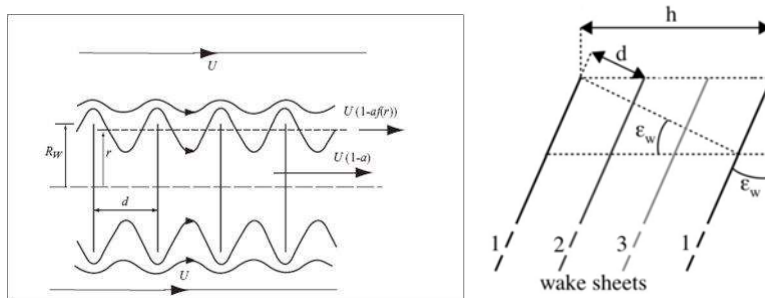


Figure 7: Left (taken from [26]): Wake model used to derive the Prandtl tip correction with  $U$  the free stream wind speed and  $d$  the distance between the vortex planes. In the right figure (modified from [28]), the angle between the helical vortex sheet and the axial direction  $\epsilon_w$  is included

Within AVATAR, see [27] the Prandtl tip loss factor has been assessed. Thereto the tip loss factor is first written in a generalized form as:

$$F = \frac{2}{\pi} \arccos[\exp(-\pi \frac{R-r_1}{d})] \quad [2]$$

With  $d$  the distance between the vortex sheets according to figure taking into account the angle between the helical vortex sheets  $\epsilon_w$

Then relation 2 is transformed to a relation which can be used in BEM based models. Thereto  $d = h/N_b \cos(\epsilon_w)$ ,  $h = 2 \pi r_2 \sin(\epsilon_w)$  and  $\epsilon_w$  is assumed to be the inflow angle at the blade element. Then the factor  $F$  can be written in the following form:

$$F = \frac{2}{\pi} \arccos[\exp(\frac{-N_b}{2} \frac{R - r_1}{r_2} \frac{\sqrt{V_n^2 + V_t^2}}{V_n})] \quad [3]$$

In equation [3]  $V_n$  is the axial velocity of wake vortices  $V_w (1-a)$  and  $V_t$  represents the tangential velocity which includes the induction in tangential direction  $\Omega r (1+a)$ .

In [27] it is then concluded that 72 variations are possible for the practical implementation of equation [3] in design codes, where knowledge is lacking on the best performing implementation.

The freedom lies in the values of  $r_1$  for which usually the local value is taken but in particular for  $r_2$  which is sometimes taken as local value but also as tip value. Moreover different implementations are possible in  $V_t$ . For the axial induction factor in  $V_n$  the local value can be used but also the tip value

where moreover a difference lies in applying the averaged value or the value at the blade section. In some cases the induction factor is even ignored.

In order to find the best choice for these factors the AWSM code is applied which has a much more physical basis to calculate the induction than the simplified wake representation from figure 7. With this code a tip loss factor is determined as the annulus average induction divided by the local induction factor. Calculations with the AWSM code have been performed for 5 different rotors, i.e. the small wind tunnel rotors from Mexico [29] (D=4.5 meter) and NREL Phase VI (D=10 meter) and the before mentioned AVATAR and INNWIND.EU rotor. Moreover a rotor has been designed as a variant of the Mexico rotor with a constant loading along the blade which is in agreement with the basic concept applied by Prandtl.

Figure 8 shows the effect of different implementation of the Prandtl tip loss factor for the constant loading variant of the Mexico rotor at a low tip speed ratios (4.9) and a high tip speed ratio (11.9) showing a large effect of the implementation.

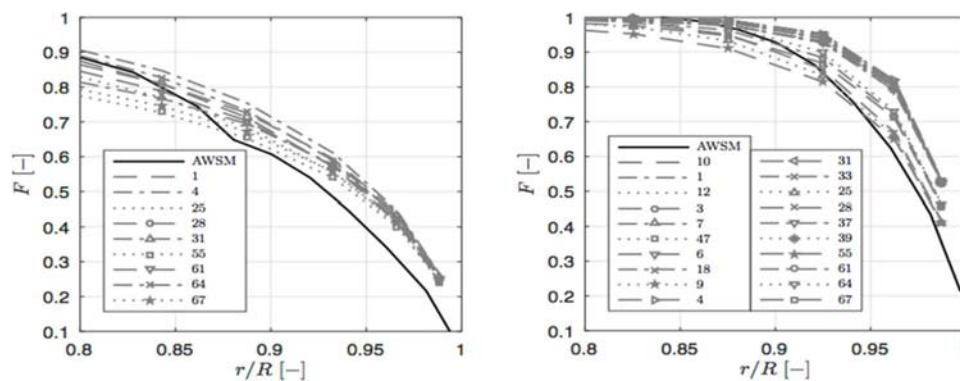


**Figure 8: Different implementation of Prandtl tip loss factor as function of radial position compared with tip loss factor from AWSM for a constant loading variant of the Mexico variant. Left:  $\lambda = 4.9$  and right  $\lambda = 11.9$**

It is then found that for all cases the best results are obtained when the distance  $r_2$  and  $V_n$  (i.e. the axial induction factor) are evaluated locally i.e. at the particular radial position of the blade element. Moreover the axial induction factor should be applied on blade level instead of on annulus averaged level. The dependency on the precise implementation of  $V_t$  turns out to be very limited.

### 3.3. How to solve the induced velocities in BEM?

A very important observation from the AVATAR project lies in the fact that the way the induction factors are solved in the BEM equations has a huge impact on the results, see [34].

This is explained through the axial BEM equation (note that similar observations can be made for the equation in tangential direction):

$$2a(1-a)\rho V_w^2 2\pi r dr = \sum_B c \frac{1}{2} \rho V_{res}^2 c_l(\alpha) \cos \phi dr [4]$$

This equation solves the axial induction factor. The axial induction factor in the momentum part (the left hand side) is straightforwardly given but it is ‘hidden’ in the blade element part (the right hand side), since the angle of attack  $\alpha$ , the resultant velocity  $V_{res}$  and the inflow angle  $\phi$  can be written in the

following form (again ignoring the tangential induction factor  $a'$  and  $\varepsilon$  denoting the twist (+pitch angle)):

$$\phi = \arctan \frac{V_w(1-a)}{\Omega r} = \arctan \frac{(1-a)}{\lambda_r}; a = \phi - \varepsilon$$

$$V_{res}^2 = V_w^2(1-a)^2 + (\Omega r)^2$$

Now consider the case of shear which gives different wind speeds throughout the annulus of figure 9 and so different wind speeds at the elements of the different blades. Then a question arises how to solve the momentum balance in this annulus. A first possibility would be to apply an **annulus approach** i.e. to average the wind speed over the annulus. Then this averaged wind speed is applied in the left hand side of equation 4 to solve the averaged induction factor. Hence in the right hand side of equation 4 the angle of attack, the inflow angle and the  $V_{res}$  are based on the averaged induction factor with the local wind speed at the blade (which in the case of shear is different from blade to blade; note that a slight complication appears by the tip loss factor which might make the local blade induction factor different from the averaged induction factor and which may even be different from blade to blade).

Another solution method would be to apply an **element approach** i.e. the axial induction factor is solved for all three blade elements separately using the local wind speed at the element. Alternatively this method may use the wind speed averaged over the sector around the blade element (figure 9). Hence the left hand side of equation 4 uses either the local wind speed or the sector averaged wind speed and the local axial induction factor at the blade. In the right hand side of equation 4 the angle of attack  $\alpha$ , the inflow angle  $\phi$  and the resultant wind speed  $V_{res}$  use the local axial induction factor as solved for each blade separately with the local wind speed at the blade element.

The aero-elastic calculations at turbulent inflow carried out with AeroModule-BEM presented in section 2 used a local approach. An overprediction in fatigue loads of approximately 15% was found. In [31] indications are found that the results from an annulus approach lead to an even larger over prediction in fatigue loads in the order of 20%. This then calls for a local approach of the induced velocity implementation. However the application of a yaw model like the one from section 3.1 requires an annulus averaged approach. This implies a dilemma when modelling yawed flow at turbulent inflow. Overall it can be stated that a generalised implementation model for the calculation of the induced velocity is needed. The definition of such approach requires further investigation.

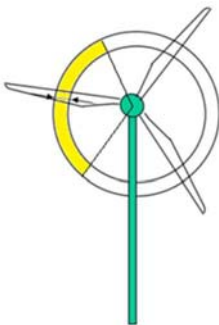


**Figure 9: Annulus ring with blade elements**

As stated above the element approach may be applied in two different ways and the question remained whether the wind speed  $V_w$  in the left hand side should be the actual wind speed at the blade element

or the sector averaged wind speed. In figure 10 a comparison is made between the induced velocities along the AVATAR blade at 4 azimuthal positions at a heavy shear with exponent 0.75 calculated with AWSM and the element approach with the local wind speed and the sector wind speed. Generally speaking the results using the sector wind speed compare better to the ASWM results.

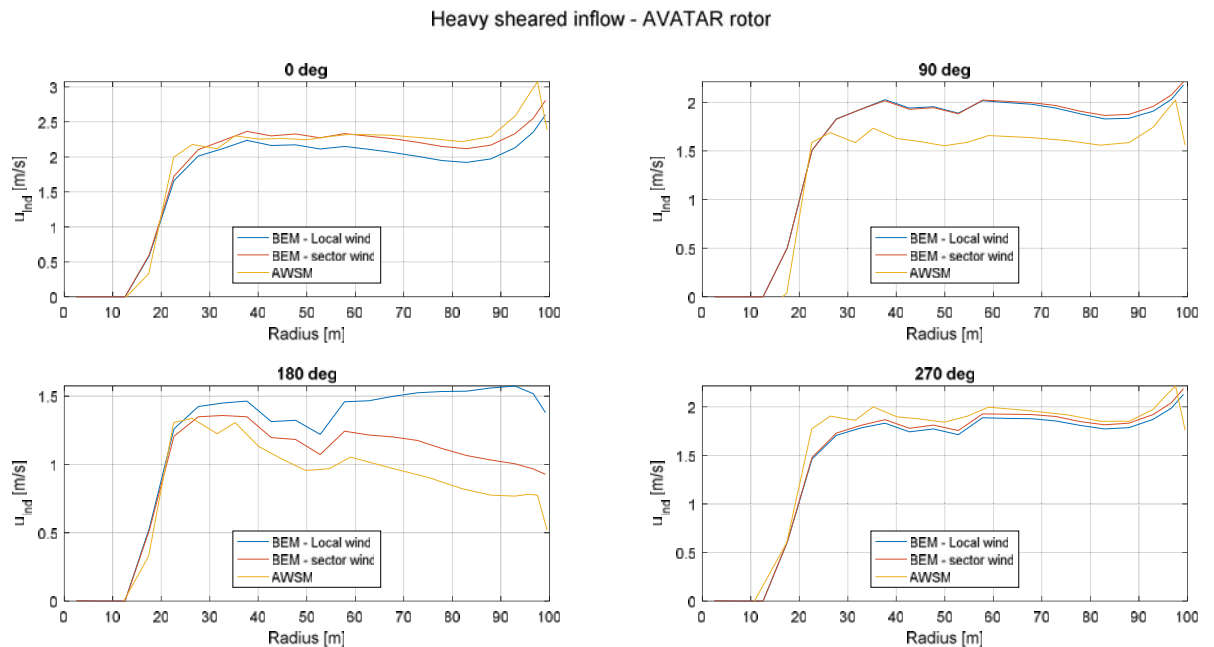


**Figure 10** Calculation with ECN's Aeromodule for the AVATAR rotor under heavy shear: induced velocity calculated with element approach and local or sector wind compared with AWSM results for 4 azimuth angles.

Hence a very important observation from the AVATAR project lies in the fact that **the** BEM model does not exist and it is not sufficient to describe a BEM model through its engineering add-ons alone, as is often done. Equally important is to describe the solution procedure for the induced velocities where an element approach is preferred for the prediction of fatigue loads under turbulent sheared inflow and an annulus approach for the prediction of yawed flow.

#### 4. Aero-elastic calculations at standstill storm cases

One of the striking observations from the AVATAR project is formed by the calculation of the aero-elastic response at standstill which showed a clear sensitivity to the precise airfoil data at post stall conditions and the modelling of dynamic stall. Simulations have been conducted for an isolated rotor and a full wind turbine in uniform as well as in turbulent inflow. In figure 11 simulations are shown on the AVATAR rotor at standstill (with blade at the 12 o' clock position) and idling at a wind speed of 48 m/s and yaw angles between -30 to +30 degrees. Minimum and maximum values of the blade root bending moment are given for turbulent inflow and for uniform inflow. For this yaw angle range the min-max difference remains limited.

Figure 12 shows the edgewise, and flapwise peak-to-peak amplitude for the AVATAR rotor calculated with different dynamic stall models and for uniform and turbulent flow. Yaw angles outside the  $\pm 30$  degree range yield extremely high loading where the ONERA dynamic stall model is found to give more damping compared to that from the Beddoes dynamic stall model. In idling conditions vibrations are reduced. Also for turbulent wind vibrations were less severe and CFD based FSI modelling also

showed significantly less vibrations even at higher yaw angles. The fact, that CFD based FSI in standstill conditions indicate a significantly more stable response than the BEM based models, is another indication that high fidelity modelling is needed, also to assist the calibration of simpler models.

More details on the studies related to aero-elastic stability and standstill conditions can be found in [32].

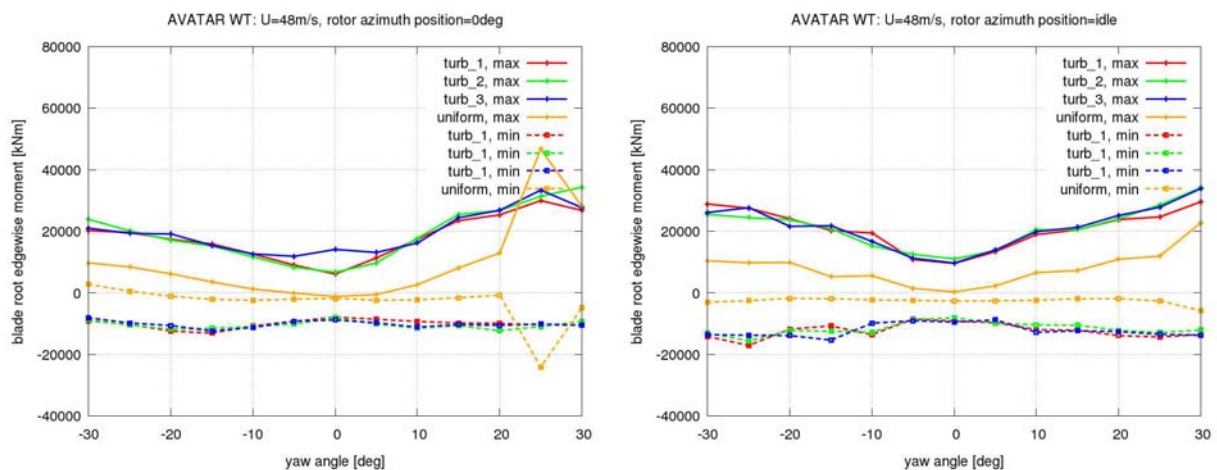


**Figure 11** Min-max values of blade root edgewise moment on the AVATAR rotor at  $U=48\text{m/s}$  in standstill (left) and idling (right) conditions.

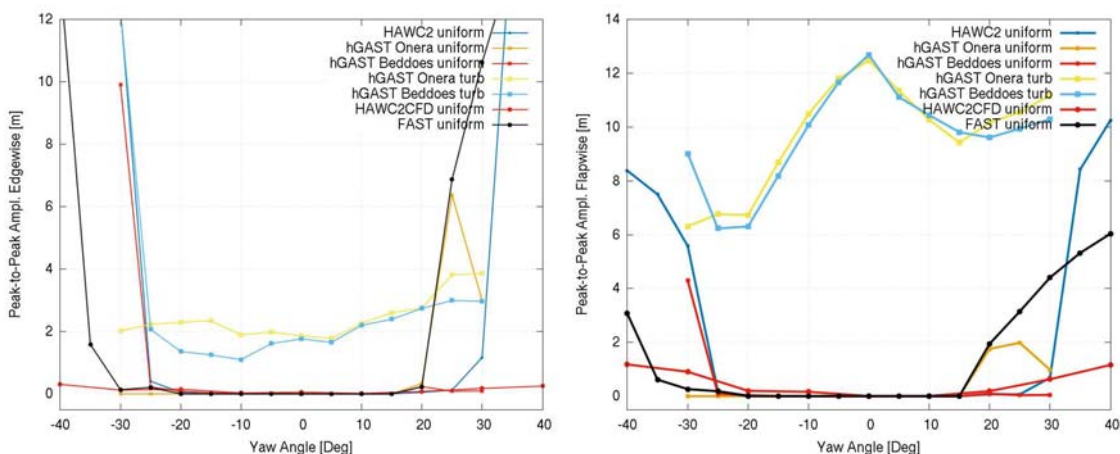


**Figure 12.** AVATAR RWT at standstill at  $48\text{m/s}$  in uniform and turbulent inflow conditions. Flapwise (right) and edgewise(left) peak-to-peak amplitude for turbulent and uniform inflow and for different dynamic stall models.

#### 4.1. 360 degrees polar

The standstill and idling results depend heavily on the precise airfoil data at deep stall. In AVATAR full 360 degrees polars have been calculated by NTUA and DTU. In this process all airfoils are studied in 2D using both the steady state and the time-accurate methods. The 2D simulations are supplemented by selected 3D DES simulations for the high angle of attack scenarios to better understand the difference between the steady and the unsteady 2D simulations. Additionally, existing measurements

performed by the University of Delft on the DU97-W-300 and DU96-W-180 airfoils at relatively low Reynolds number were compared to both 2D RANS and 3D DES simulations. It was found that the steady RANS simulations clearly under predict the drag in deep stall where the unsteady RANS clearly over predicts drag. A few simulations are performed using the much more expensive 3D unsteady IDDES simulations. The 3D DES simulations reduce to the standard  $k - \omega$  SST results in the attached flow regions, and the expensive simulations are done only for the regions where the 2D simulations experience problems. From the results it is seen that a very good agreement with measurements is found in the stalled regions, see Figure 13 and [33]. The problematic areas left are

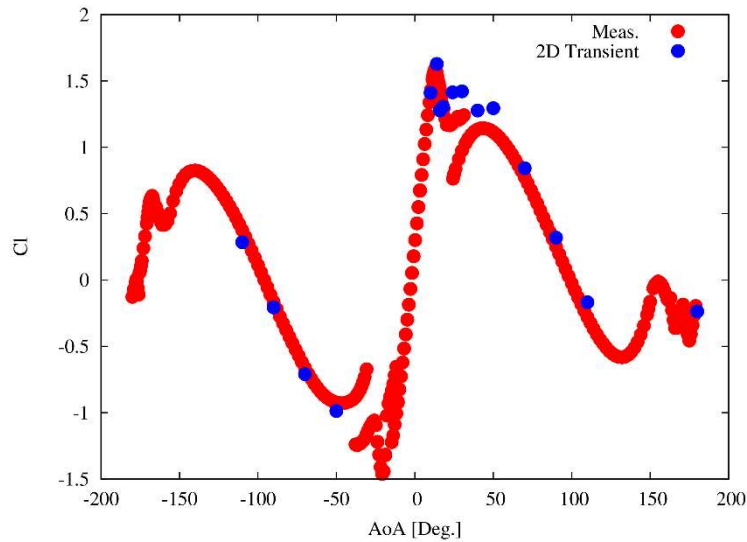


**Figure 13.** Comparison between lift for the DU97-W-300 measured in the Delft LSLT tunnel and 3D CFD computations using IDDES technique in the DTU's EllipSys3D

close to the onset of stall, while the deep stall regions seems to be well captured.

## 5. Conclusions

The present paper presents results from the recently finished AVATAR project. This project has led to a huge number of publicly available results. Amongst others all deliverables, including the final report, are uploaded on <http://www.eera-avtar.eu/publications-results-and-links/>

In this paper special attention is paid to 1) the improvement and assessment of low fidelity engineering (BEM based) models with intermediate fidelity free vortex wake (FVW) models and 2) to the prediction of standstill conditions at storm wind speeds

With regard to the first subject the following conclusions were drawn:

- Generally speaking the load cases which are determined by induction effects (e.g. yawed cases) are more challenging to model by BEM based methods than the cases driven by the external flow field (e.g. sheared cases). Such cases driven by induction effects were modelled quite accurately with intermediate fidelity free vortex wake (FVW) methods in a relatively efficient way.
- Fatigue loads for normal production cases at turbulent inflow were over predicted with approximately 15% or more by BEM models compared to results from FVW methods possibly by a more local tracking of induced velocities in FVW methods
- Results from FVW models could be used to improve lower fidelity models for e.g. the prediction of yaw and tip losses.
- The outcome of BEM based models does not only depend on the choice of engineering add-ons (as is often assumed) but it is also heavily dependent on the way how the induced velocities are



solved. To this end an annulus and an element approach were assessed with the aid of FVW methods. For the prediction of fatigue loads the so-called element approach is recommended but for the modelling of yaw an annulus approach is preferred. The combined calculation of yaw at turbulent inflow then pleads for a generalised solution method for the induced velocities

- The experiences gained with FVW methods coupled to an aero-elastic solver have paved the way to model (a limited number of) load cases in a design spectrum more reliable but still relatively efficient with such methods. This is in particular promising for load cases in which induction effects are expected to be dominant.

With regard to the second subject (aero-elastic stability at **standstill storm** conditions) the following conclusions were drawn

- Dependant on the dynamic stall model and the deep stall airfoil data a stable or instable situation is predicted. This implies that state of the art methods cannot predict aero-elastic stability with certainty
- For the prediction of deep stall airfoil data DES models were shown to give promising results.

Finally it is concluded that, although AVATAR's strategy to improve lower fidelity models with higher fidelity models was very successful, the experimental validation basis was considered too limited by the project group. High quality **measurements** are urgently needed in both the field and the wind tunnel.

### Acknowledgement

The project AVATAR received funding from the European Union's Seventh programme for research, technological development and demonstration under Grant Agreement NO FP7-ENERGY-2013-1/no 608396.

### References

- [1] Bak, C., Zahle, F., Bitsche, R., Kim, T., Yde, A., Henriksen, L., Hansen MH, Blasques JPAA, Gaunaa MA. Natarajan, M. H. *The DTU 10-MW Reference Wind Turbine* Danish Wind Power Research 2013, Fredericia, Denmark, 27/05/2013
- [2] G. Sieros, D. Lekou, D. Chortis, P. Chaviaropoulos, X. Munduate, A. Irisarri, H. Aa. Madsen, K. Yde, K. Thomsen, M. Stettner, M. Reijerkerk, F. Grasso, R. Savenije, G. Schepers, C.F. Andersen *AVATAR Reference Blade Design, AVATAR Deliverable 1.2*, <http://www.eera-avатар.eu/> January 2015
- [3] O Pires, X Munduate, O Ceyhan, M Jacobs, H Snel *Analysis of high Reynolds numbers effects on a wind turbine airfoil using 2D wind tunnel test data* Science of Making Torque 2016,
- [4] H. Heißelmann, J. Peinke, M. Hölling *Experimental airfoil characterization under tailored turbulent conditions* Science of Making Torque 2016
- [5] C. Ferreira, *Results of the AVATAR project for the validation of 2D aerodynamic models with experimental data of the DU95W180 airfoil with unsteady flap* Science of Making Torque, October 2016
- [6] D Baldacchino, M Manolesos, C Ferreira, A Gonzalez Salcedo, M Aparicio, T Chaviaropoulos, K Diakakis, L Florenti, N R. Garcia, G Papadakis, N N. Sørensen, N Timmer, N Troldborg, S Voutsinas and A van Zuijlen *Experimental benchmark and code validation for airfoils equipped with passive vortex generators*, Science of Making Torque, October 2016
- [7] Madsen, H. A., Bak, C., Paulsen, U. S., Gaunaa, M., Sørensen, N. N., Fuglsang, P., Jensen, L. (2010). *The DAN-AERO MW experiments*. 48th Aiaa Aerospace Sciences Meeting Including the New Horizons Forum and Aerospace Exposition, 2010–0645.
- [8] A. Gonzalez, D. Baldacchino, M. Caboni, A. Kidambi M. Manolesos, N. Troldborg *Aerodynamic flow control: final report*, Deliverable D3.5, October 2016

- [9] N. Sørensen, B. Mendez, A. Munoz, G. Sieros, E. Jost, T. Lutz, G. Papadakis, S. Voutsinas, G. Barakas, S. Colonia, D. Baldacchino, C. Baptista, C. Ferreira *CFD comparison for 2D flow* Science of Making Torque, October 2016
- [10] N.N. Sørensen, A. Gonzalez Salcedo, R. Martin, E. Jost, G. Pirrung, H. Rahimi, G. Schepers, G. Sieros, H.A. Madsen, K. Boorsma, N. Ramos Garcia, S. Voutsinas, T. Lutz *Engineering models for complex inflow situations*, Deliverable D2.8, October 2017
- [11] H. Rahimi, J.G. Schepers, W.Z. Shen, N. Ramos García, M.S. Schneider, D. Micallef, C.J. Simao Ferreira, E. Jost, L. Klein, I. Herráez *Evaluation of different methods for determining the angle of attack on wind turbine blades with CFD results under axial inflow conditions* Renewable Energy. 125. 10.1016/j.renene.2018.03.018., 2018
- [12] Sørensen, N. N.: *General purpose flow solver applied to flow over hills*, Tech. rep., Risø, [http://www.citeulike.org/user/pire\\_1024/article/5890204](http://www.citeulike.org/user/pire_1024/article/5890204), 1995.
- [13] van Garrel A. Development of a wind turbine aerodynamics simulation module, Energy Research Centre of the Netherlands, ECN", ECN-C--03-079, August, 2003
- [14] H Aa Madsen, T J Larsen, G R Pirrung, and D R Verelst. An implementation of the BEM model for simulation of non-uniform loading and inflow. To be submitted.
- [15] G. R. Pirrung, H. A. Madsen, T. Kim, and J. Heinz. *A coupled near and far wake model for wind turbine aerodynamics*. Wind Energy, 2016. doi:10.1002/we.1969.
- [16] Boorsma, K.; Grasso, F.; Holierhoek, J.G. *Enhanced approach for simulation of rotor aerodynamic loads*, ECN-M--12-003, 2012
- [17] C. Lindenburg *Comparison of PHATAS Versions and the Wind turbine Module* ECN-E--11-066, 2011
- [18] J.G. Schepers O. Ceyhan and K. Boorsma and A. Gonzalez and X Munduate and O Pires and N.. Sørensen and C. Ferreira and G Sieros and J. Madsen and S. Voutsinas and T. Lutz and G. Barakos and S. Colonia and H. Heißelmann and F. Meng and A. Croce *Latest results from the EU project AVATAR: Aerodynamic modelling of 10 MW wind turbines* Science of Making Torque conference 2017
- [19] H. Rahimi and M. Hartvelt and J. Peinke and J.G Schepers *Investigation of the current yaw engineering models for simulation of wind turbines in BEM and comparison with CFD and experiment* Science of Making Torque 2016
- [20] J.G. Schepers and H. Snel *Final results of the EU project Dynamic Inflow*, Presented at ASEM Energy Week, January 1996
- [21] J.G. Schepers *An engineering model for yawed conditions developed on basis of wind tunnel measurements*, In proceedings of ASME Wind Energy Symposium held at Reno USA, January 1999
- [22] J.G. Schepers *Engineering models in aerodynamics*, PhD thesis, November 27<sup>th</sup>, 2012, Technical University of Delft, Netherlands, ISBN [9789461915078](https://doi.org/10.1007/978-94-6191-507-8)
- [23] NWTc information portal (SOWFA) - simulator for wind farm applications <https://nwtc.nrel.gov/SOWFA>
- [24] H. Rahimi A.M. Garcia, B. Stoevesandt, J. Peinke and J.G Schepers *A new engineering model for simulation of wind turbines in BEM at yawed conditions*, Journal of Wind Energy, 2018
- [25] Shen W.Z., Mikkelsen R., Sorensen J.N. and Bak C *Tip loss corrections for wind turbine computations*, Journal of Wind Energy 2005;8:457-475, March 2005,
- [26] Burton T., Sharpe D., Jenkins N., Bossanye E *Wind Energy Handbook*, John Wiley and Sons, 2001
- [27] Ramdin, S.F.. *Prandtl tip loss factor assessed*, ECN-Wind-2017-023, February 2017
- [28] E. Branlard *Wind Turbine Aerodynamics and Vorticity-Based Methods*, Springer, 2017
- [29] J. G. Schepers and H. Snel. (2008). *'Model Experiments in Controlled Conditions, Final report.'* ECN-E-07-042, Energy Research Center of the Netherlands, ECN. <http://www.ecn.nl/publicaties/default.aspx?nr=ECN-E--07-042>.
- [30] S. Schreck. (2008). *IEA Wind Annex XX: HAWT Aerodynamics and Models from Wind Tunnel*

- Measurements*. TP-500-43508, National Renewable Energy Laboratory, Golden, Colorado.  
<http://www.nrel.gov/docs/gen/fy09/43508.pdf>
- [31] K. Boorsma, P. Chasapogiannis, D. Manolas, M. Stettner, M. Reijerkerk *Comparison of models with respect to fatigue load analysis of the Innwind.EU and Avatar RWT's*, Deliverable 4.6, September 2016
- [32] J. Heinz, N.N. Sørensen, V. Riziotis, P. Chassapoyannis, C.M. Schwarz, S. Gomez Iradi, M. Stettner *Stand-still operation*, Deliverable 4.5, August 2016
- [33] N.N. Sørensen and W.A. Timmer *CFD prediction of airfoil deep stall performance using Improved Delayed Detached Eddy Simulations*, Presented at: Wind Energy Science Conference 2017, June 2017, Lyngby
- [34] H. Aa. Madsen et. al., *Blade element momentum modeling of inflow with shear in comparison with advanced model results*, WIND ENERGY, 2012
- [35] J.G. Schepers et al. AVATAR Project Final report <http://www.eera-avatar.eu/publications-results-and-links/>, February 2018
- [36] I. Herráez, I., Daniele, E., and Schepers, J. G.: Extraction of the wake induction and angle of attack on rotating wind turbine blades from PIV and CFD results, *Wind Energ. Sci.*, 3, 1-9, <https://doi.org/10.5194/wes-3-1-2018>, 20